Available online at www.jbr-pub.org.cn

Open Access at PubMed Central

The Journal of Biomedical Research, 2020 34(4): 251–254

JBR

Supplementary Data

Tyrosyl radical in haemoglobin and haptoglobin-haemoglobin complex: how does haptoglobin make haemoglobin less toxic?

Dimitri A. Svistunenko[1,✉], Andreea Manole[2]

[1]*Biomedical EPR Facility, School of Life Sciences, University of Essex, Colchester, Essex CO4 3SQ, UK;*
[2]*Laboratory of Genetics, The Salk Institute for Biological Studies, La Jolla, CA 92037, USA.*

Updated TRSSA - what is new?

Tyrosyl Radical Spectra Simulation Algorithm (TRSSA)[1] uses two input parameters, spin density on atom C1 ρ_{C1} and phenoxyl ring rotation angle θ (***Supplementary Fig. 1***), to calculate all parameters needed for simulation of a Tyr radical EPR spectrum. Euler angles for the methylene β-protons hyperfine interaction tensors were set to zeros in the original TRSSA. We now used Density Function Theory (DFT) calculations to determine the Euler angles for the protons as functions of the ring rotation angle θ.

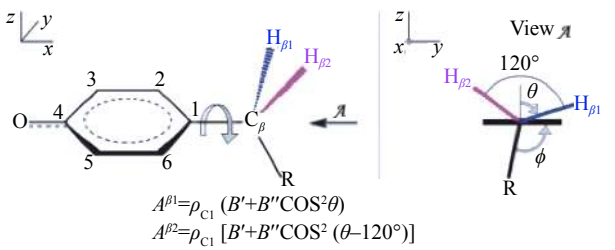

Supplementary Fig. 1 **Tyrosyl radical, the Cartesian coordinate system (right-handed) aligned with the principal g -factor value directions and the definition of the phenoxyl ring rotation angle.** The hyperfine interaction constants A for the methylene protons β1 and β2 are proportional to the spin density ρ_{C1} on atom C1 and depend on θ according to the McConnell relationship (B' and B'' are constants) [2]. Angle φ is an alternative definition of the ring rotation, more practical for crystal structure analysis, when H-atoms are not visible.

DFT calculation of Euler angles for a model Tyr radical

DFT was used to determine the Euler angles for the β-protons in a model Tyr radical for two rotational conformations of the ring, with θ=30° and θ=60° (***Supplementary Fig. 2***).

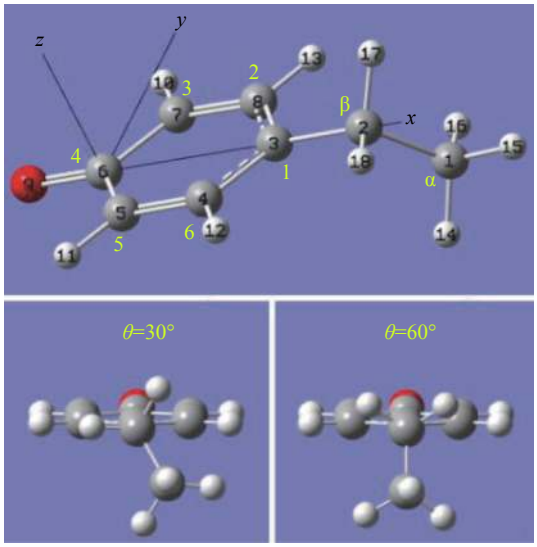

Supplementary Fig. 2 **The Tyr model and two ring conformations analysed.** At the top: the model Tyr radical used in the DFT calculations. Atom numbers assigned by Gaussian are indicated (in a smaller font on the atoms) along with traditional atom nomenclature in a tyrosine (in a bigger font by the atoms). At the bottom: the model at two different conformations, with the ring rotation angles θ=30° and θ=60°, shown for view A as define in ***Supplementary Fig. 1***.

✉Corresponding author: Dimitri A. Svistunenko, Biomedical EPR Facility, School of Life Sciences, University of Essex, Colchester, Essex CO4 3SQ, UK. Tel/Fax: +441206 873149/+441206 872592, E-mail: svist@essex.ac.uk.

Received 08 September 2018, Revised 27 November 2018, Accepted 01 March 2019, Epub 15 May 2019

CLC number: R457.1, Document code: A

The authors reported no conflict of interests.

https://doi.org/10.7555/JBR.33.20180084

Gaussian03 package[3] was used for both the optimisations of the structures and the calculation of the EPR parameters, both at the B3LYP/6-31G* level of theory. During the optimization, the atom coordinates that define the rings rotation angles were kept frozen. After optimization, the Cartesian axes, changed by the optimisation process, have been re-assigned as shown in ***Supplementary Fig. 2***. This was done by using ArgusLab 4.0.1[4] as follows. Ox was first set through C6-C2 (Gaussian nomenclature); Oy was then linked to C6-C7, that moved Ox away from the C6-C2 direction but set Oz perpendicular to the ring plane. Now Ox was re-aligned to C6-C2 which moved Oy away from C7 but did keep it within the ring plane. Single point calculations were then performed with the *NoSymm* keyword to prevent molecule re-orientation. The Gaussian output files for the two single point calculations are available in the *Supplementary theta_30_degrees.out* and *theta_60_degrees.out* (all the supplementary files are available on: https://1drv.ms/u/s!ArZmAEA-E2XThrNQz79qUXuUqIrL-A?e=4fNPKw).

Euler angles *Φ1*, *Φ2* and *Φ3* for a proton's *A*-tensor were calculated from the projections of three unity vectors, aligned with the directions *aa*, *bb* and *cc* of the Anisotropic Spin Dipole Coupling components, onto Cartesian axes x, y and z. These projections are available in the Gaussian output, and the *A-values_and_Euler_angles* spreadsheet of *Supplementary Euler_angles.xlsx* was used to perform the calculations. This Excel file was adapted from the file published in the Electronic Supplementary Information to our work published previously[5]. Attention has been paid to the choice of left and right Cartesian coordinate systems and to different definition of the coupling constants in Gaussian (B_{aa} - smallest, B_{bb} - intermediate, B_{cc} - highest) and in SimPow6 ($|A_{aa}|$ - smallest, $|A_{bb}|$ - intermediate, $|A_{cc}|$ - highest-by absolute value). The three Euler angles are defined as follows:

•First rotation *Φ1* is around *z* when *z* is directed towards the observer, to bring A_{cc} to the *zx* plane.

•Second rotation *Φ2* is around *y* when *y* is directed away from the observer, to align A_{cc} with *x*.

•Third rotation *Φ3* is around *x* when *x* is directed towards the observer; *Φ3* is positive when measured counter clock-wise from positive direction of *y*.

The formulae for the calculation of the Euler angles can be viewed by selecting appropriate cells on *A-values_and_Euler_angles* spreadsheet and are derived on the *Euler_angles_explained* spreadsheet of *Supplementary Euler_angles.xlsx*.

Euler angles for a rotational orientation of the ring between 30° and 60°

In TRSSA2, the Euler angles for a specific ring

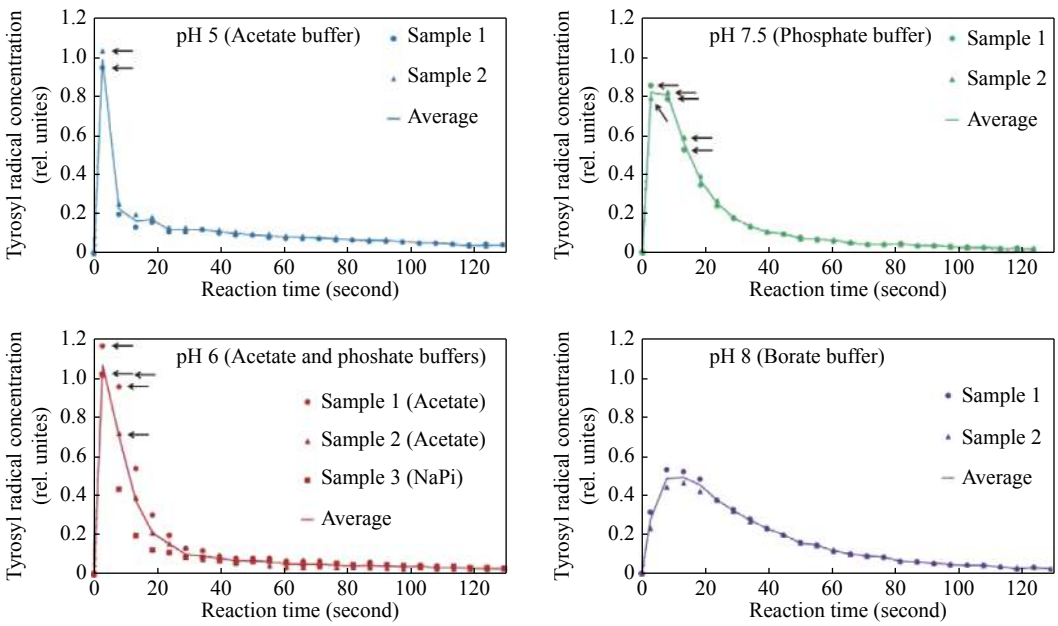

Supplementary Fig. 3 **Kinetic dependences of the tyrosyl radical in the individual samples of 340 μmol/L metHb mixed with a 4-fold excess of H_2O_2 (1.36 mmol/L, both concentrations are final), at the range of pH values of pH 5–pH 8 maintained by different buffers.** Averaged data (lines) for the four pH values are shown on one graph in ***Fig. 3*** as data points. The thirteen EPR spectra corresponding to the data points marked with arrows have been averaged to produce the spectrum in inset in ***Fig. 3***. The nine first spectra of Sample 1 at pH 7.5 (up to 45 seconds) are shown in ***Fig. 1***.

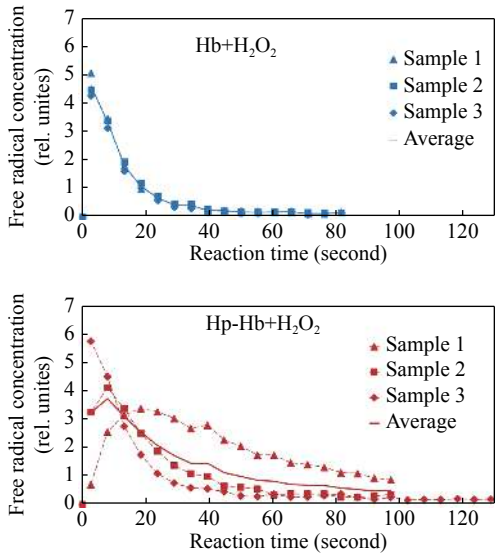

Supplementary Fig. 4 **Kinetic dependences of the free radical in three similar experiments of mixing 130 μmol/L Hb with 1.558 mmol/L H_2O_2 and in three similar experiments of mixing 130 μmol/L Hp-Hb with 1.558 mmol/L H_2O_2, at pH 7.4.** The averaged data (solid lines) are plotted on one graph in ***Fig. 5***. Note that while the kinetics of the free radical in unbound Hb are very close in the three similar experiments, this is not so for the Hp-Hb complex: the three similar Hp-Hb+H_2O_2 experiments exhibit rather different kinetics. While the cause of this variability should be investigated in the future works, such kinetic behavior seems to be the reason for rather different relative increase of the free radical yield in the Hp-Hb complex, as compared to unbound Hb, observed before in the frozen samples[6–7].

rotational conformation θ, which is within the interval of $30° \leqslant \theta \leqslant 60°$, were calculated as linear interpolation of the DFT determined values for θ=30° and θ=60°. This interval of θ was selected because the original TRSSA has yielded this angle to be 53° in the human Hb radical[1] and because this angle was estimated as 47° in the Hp-Hb complex[6]. Thus the angle in both free and Hp-bound Hb was expected to be within the 30°–60° interval.

EPR spectra simulation parameters

The parameters used to simulate the free radical EPR spectra of Hb and Hp-Hb complex were generated by TRSSA2 and are summarized in ***Supplementary Table 1*** and ***Table 2***, respectively. The SimPow6 input data files (*Supplementary d_Hb.dat* and *d_Hb_Hp.dat*) were based on these tables.

Supplementary Table 1 **Parameters used to simulate the Hb free radical EPR spectrum (*Fig. 6*) – a TRSSA output for an input of ρ_{C1}=0.405 and θ=53.0°**

g_x	g_y	g_z			
2.00707	2.00421	2.00221			
Hyperfine coupling matrix principal values			Euler angle α	Euler angle β	Euler angle γ
$A_{cc}^{\beta 1}$, MHz	$A_{bb}^{\beta 1}$, MHz	$A_{aa}^{\beta 1}$, MHz	$-\Phi_1^1$, degree	$-\Phi_2^1$, degree	$-\Phi_3^1$, degree
24.19	20.70	20.70	–23.1	–11.5	–39.6
$A_{cc}^{\beta 2}$, MHz	$A_{bb}^{\beta 2}$, MHz	$A_{aa}^{\beta 2}$, MHz	$-\Phi_1^2$, degree	$-\Phi_2^2$, degree	$-\Phi_3^2$, degree
12.28	7.68	7.68	25.4	–6.7	–41.8
A_{cc}^{C3}, MHz	A_{bb}^{C3}, MHz	A_{aa}^{C3}, MHz	$-\Phi_1^{C3}$, degree	$-\Phi_2^{C3}$, degree	$-\Phi_3^{C3}$, degree
–25.9	–8.1	–20.5	23.0	0.0	0.0
A_{cc}^{C5}, MHz	A_{bb}^{C5}, MHz	A_{aa}^{C5}, MHz	$-\Phi_1^{C5}$, degree	$-\Phi_2^{C5}$, degree	$-\Phi_3^{C5}$, degree
–25.9	–8.1	–20.5	–23.0	0.0	0.0
A_{cc}^{C2}, MHz	A_{bb}^{C2}, MHz	A_{aa}^{C2}, MHz	$-\Phi_1^{C2}$, degree	$-\Phi_2^{C2}$, degree	$-\Phi_3^{C2}$, degree
7.5	5.0	1.5	40.0	0.0	0.0
A_{cc}^{C6}, MHz	A_{bb}^{C6}, MHz	A_{aa}^{C6}, MHz	$-\Phi_1^{C6}$, degree	$-\Phi_2^{C6}$, degree	$-\Phi_3^{C6}$, degree
7.5	5.0	1.5	–40.0	0.0	0.0
ΔH_x, Gauss	ΔH_y, Gauss	ΔH_z, Gauss			
6.38	4.68	4.43			

Orange indicates radical parameters generated by the algorithm for an input of ρ_{C1} and θ; Light blue indicates conserved parameters (the same for all Tyr radicals).

Supplementary Table 2 **Parameters used to simulate the Hp-Hb free radical EPR spectrum (*Fig. 6*) – a TRSSA output for an input of ρ_{C1}=0.360 and θ=54.3°**

g_x	g_y	g_z			
2.00868	2.00435	2.00215			
Hyperfine coupling matrix principal values			Euler angle α	Euler angle β	Euler angle γ
$A_{cc}^{\beta 1}$, MHz	$A_{bb}^{\beta 1}$, MHz	$A_{aa}^{\beta 1}$, MHz	$-\Phi_1^1$, degree	$-\Phi_2^1$, degree	$-\Phi_3^1$, degree
20.34	17.23	17.23	–23.4	–10.9	–38.6
$A_{cc}^{\beta 2}$, MHz	$A_{bb}^{\beta 2}$, MHz	$A_{aa}^{\beta 2}$, MHz	$-\Phi_1^2$, degree	$-\Phi_2^2$, degree	$-\Phi_3^2$, degree
11.71	7.77	7.77	25.4	–6.9	–43.9
A_{cc}^{C3}, MHz	A_{bb}^{C3}, MHz	A_{aa}^{C3}, MHz	$-\Phi_1^{C3}$, degree	$-\Phi_2^{C3}$, degree	$-\Phi_3^{C3}$, degree
–25.9	–8.1	–20.5	23.0	0.0	0.0
A_{cc}^{C5}, MHz	A_{bb}^{C5}, MHz	A_{aa}^{C5}, MHz	$-\Phi_1^{C5}$, degree	$-\Phi_2^{C5}$, degree	$-\Phi_3^{C5}$, degree
–25.9	–8.1	–20.5	–23.0	0.0	0.0
A_{cc}^{C2}, MHz	A_{bb}^{C2}, MHz	A_{aa}^{C2}, MHz	$-\Phi_1^{C2}$, degree	$-\Phi_2^{C2}$, degree	$-\Phi_3^{C2}$, degree
7.5	5.0	1.5	40.0	0.0	0.0
A_{cc}^{C6}, MHz	A_{bb}^{C6}, MHz	A_{aa}^{C6}, MHz	$-\Phi_1^{C6}$, degree	$-\Phi_2^{C6}$, degree	$-\Phi_3^{C6}$, degree
7.5	5.0	1.5	–40.0	0.0	0.0
ΔH_x, Gauss	ΔH_y, Gauss	ΔH_z, Gauss			
4.25	2.79	2.71			

Orange indicates radical parameters generated by the algorithm for an input of ρ_{C1} and θ; Light blue indicates conserved parameters (the same for all Tyr radicals).

References

[1] Svistunenko DA, Cooper CE. A new method of identifying the site of tyrosyl radicals in proteins[J]. *Biophys J,* 2004, 87(1): 582–595.

[2] McConnell HM, Chesnut DB. Theory of isotropic hyperfine interactions in π-electron radicals[J]. *J Chem Phys,* 1958, 28(1): 107–117.

[3] Frisch MJ, Trucks GW, Schlegel HB, et al. Gaussian 03. revision E.01[M]. Wallingford: Gaussian, Inc., 2004.

[4] Thompson M. ArgusLab 4.0.1. Seatle: planaria software, LLC, 2014[EB/OL].[2010-11-01]. http://www.arguslab.com/arguslab.com/Welcome.html.

[5] Svistunenko DA, Jones GA. Tyrosyl radicals in proteins: a comparison of empirical and density functional calculated EPR parameters[J]. *Phys Chem Chem Phys,* 2009, 11(31): 6600–6613.

[6] Cooper CE, Schaer DJ, Buehler PW, et al. Haptoglobin binding stabilizes hemoglobin ferryl iron and the globin radical on tyrosine β145[J]. *Antioxid Redox Signal,* 2013, 18(17): 2264–2273.

[7] Mollan TL, Jia YP, Banerjee S, et al. Redox properties of human hemoglobin in complex with fractionated dimeric and polymeric human haptoglobin[J]. *Free Radic Biol Med,* 2014, 69: 265–277.